Catalysis Today 171 (2011) 60–66

Contents lists available at ScienceDirect

Catalysis Today

journal homepage: www.elsevier.com/locate/cattod

CH_4 decomposition on Ni and Co thin layer catalysts to produce H_2 for fuel cell

F. Frusteri[a,b,*], G. Italiano[b], C. Espro[b], F. Arena[a,b]

[a] Institute CNR-ITAE, Via S. Lucia 5, 98126 Messina, Italy
[b] Messina University, Dept of Industrial Chemistry, Salita Sperone 31 - 98166 S. Ágata, Messina, Italy

ARTICLE INFO

Article history:
Received 4 November 2010
Received in revised form 21 February 2011
Accepted 9 March 2011
Available online 13 April 2011

Keywords:
Methane decomposition
Hydrogen
Thin layer catalyst
Multilayer reactor

ABSTRACT

Ni and Co supported on SiO_2 and Al_2O_3 Silica Cloth Thin Layer Catalysts (TLC) were investigated in the Catalytic Decomposition of Natural Gas (CDNG) reaction using a Multilayer Catalytic Reactor (MCR). The influence of support and reaction temperature was evaluated with the aim to design a novel catalyst suitable to develop a dual-step process to produce pure hydrogen for fuel cell. Ni and Co silica supported catalyst, due to the low metal supported interaction (MSI) characterizing such systems, were not found suitable to efficiently perform CDNG reaction. On the contrary in case alumina was used as support both metals strongly interact with surface becoming so more resistant to sintering. In addition in case the metals (both Ni and Co) strongly interact with support surface, the formation of encapsulating carbon is depressed and only filamentous carbon forms. Using Ni and Co TLC supported on Al_2O_3 samples it has been possible to realize a cyclic dual-step process based on reaction and regeneration in oxygen stream without any catalyst detriment.

A deactivation modelling to discriminate the role of sintering and coking on the deactivation pattern is proposed.

1. Introduction

Today the worldwide production of hydrogen (500 billion Nm^3/y) comes from fossils feedstock by mature technologies which however should be improved in terms of economic and energy efficiency. Around 190 millions/y of hydrogen represent a by-product of the chemical industry (es. Chlorine-Soda technologies) [1,2], while the rest derives from fossil feedstocks (natural gas, heavy oil, coal) through reforming, oxidation or gasification processes.

If attention is focused on the use of hydrogen as clean fuel to produce energy by fuel cell systems, the development of an efficient catalytic process for the production of "CO_x-free" H_2 is important in order to overcome hurdles associated with the use of a conventional multi-step process. In this context, a reversible cyclic stepwise process based on catalytic decomposition of natural gas (CDNG) and carbon removal could represent a suitable technology for small scale hydrogen production for fuel cell application [3]. The catalytic decomposition of natural gas (CDNG) into hydrogen and carbon is attracting much research interest since it appears to be a direct, mildly endothermic, attractive way for producing highly "pure" hydrogen with reduced CO_2 emissions [4]. Although the CDNG reaction was extensively studied in the last decades [5], the main technological drawbacks associated with catalyst lifetime and regeneration remain still unsolved [5]. Ni-based systems are the most investigated systems since they are active and stable at mild reaction conditions (T_R, 773–873 K; P_R, 0.1 MPa) [6–11]. Unfortunately, their use has met some drawbacks since they are active in a very narrow window of working temperature [12,13] and are unstable during oxidative treatment (burn-off with O_2/air, gasification with H_2O/CO_2) normally used for coke removal [12,13]. Furthermore, the thermodynamic restrictions impose the adoption of high reaction temperatures (>873 K) in order to attain high CH_4 conversion values [3,5], ruling out the practical application of nickel based catalysts, which are very active in the CDNG reaction under mild reaction conditions (773–873 K) [14]. Recent studies have documented that Co based catalysts could exhibit a superior performance in CDNG at high T_R (773–1073 K) [15].

The cobalt-based catalysts have been object of several studies in the CDNG reaction [16,17]. At temperatures higher than 873 K in CH_4 atmosphere the cobalt catalysts promote the formation of "single walled nano-tube "(SWNT) [18]. Although the Co catalysts are less active with respect to the Nickel catalysts, they result to be interesting from an economical point of view with respect to the Nickel ones. Furthermore, considering that Co catalysts could promote the SWNT formation without detachment of particles from the support, processes based on reaction/regeneration steps (burn-off, CO_2/H_2O gasification) could be developed [19,20]. The Co-based systems denote the best performances both in terms of H_2 productivity and of selectivity to SWNT when supported on Al_2O_3 carrier. Cobalt particles strongly adsorb on Al_2O_3 support giving rise to

* Corresponding author.
E-mail address: francesco.frusteri@itae.cnr.it (F. Frusteri).

0920-5861/$ – see front matter © 2011 Elsevier B.V. All rights reserved.
doi:10.1016/j.cattod.2011.03.016

Table 1
Chemical–physical properties of Ni and Co TLCs.

Sample	Composition	Metal loading (%)	SA_{BET} (m^2/g)	MSA (m^2 Me/g)	D (%)	d_s (nm)
20NiAS	Ni/Al_2O_3/cloth	19.6	45.4	1.7	5.9	17.2
20CoAS	Co/Al_2O_3/cloth	18.4	46.0	1.6	5.5	18
20NiS	Ni/SiO_2/cloth	19.5	51.0	3.6	7.1	14
20CoS	Co/SiO_2/cloth	17.8	63.0	1.8	3.0	6.0
MNi	Mg–Ni/SiO_2/cloth	5.0/20.5	42.7	5.8	10.8	9.3
20Co5MoAS	Co–Mo/Al_2O_3/cloth	15.9/5.0	12.4	1.8	5.5	18

the formation of $CoAl_2O_4$–type structures, which ensure an elevated metal dispersion inhibiting also the occurrence of sintering phenomena [21,22].

This paper is aimed to compare the behaviour of Ni and Co thin layer catalysts in the Catalytic Decomposition of Natural Gas (CDNG) to produce CO_x "free" H_2 stream suitable to be used in the fuel cell technology. The feasibility of a reversible two-step process for based on CDNG and carbon removal is outlined.

2. Experimental

2.1. Catalyst preparation

A commercial silica fabric (OS 120,Thermal Material Systems (TMS) product; thickness, 0.15 mm; specific weight, 120 g/m^2) was wash-coated with a dispersion of Al_2O_3 (Disperal P2, Sasol product; SA_{BET}, 260 m^2 g^{-1}) in order to confer an adequate surface area for the dispersion of the active species. After the wash coating procedure the samples were dried in air at 393 K for 12 h and shaped in circular form (Ø, 37 mm).

Ni and Co supported on Al_2O_3/Silica cloth samples (NiAS and CoAS) were prepared by incipient wetness (Al_2O_3/Silica cloth) using a 0.1 M aqueous solution of Ni and Co nitrates. After each impregnation the samples were dried in air at 393 K for 12 h and further calcined in air at 873 K for 3 h.

The MgO modified Ni/SiO_2/cloth sample was prepared by co-impregnation of the SiO_2/silica cloth support with an aqueous solution of $Ni(NO_3)_2$ and $Mg(NO_3)_2$. After impregnation the sample was dried at 393 K for 12 h and further calcined in air at 873 K for 3 h.

Co–Mo/Al_2O_3/silica cloth sample with cobalt loading of 20% and Mo loading of 5% was prepared by soaking co-impregnation method.

2.2. Catalyst characterization

Surface Area (SA_{BET}), Pore Volume (PV) and the Pore Size Distribution (PSD) were determined from the nitrogen adsorption/desorption isotherms, using an ASAP 2010 (Micromeritics Instrument) gas adsorption device. Before analysis, all the samples were outgassed at 423 K under vacuum (2 h).

H_2-TPD measurements in the range 193–923 K, to evaluate the H_2 uptake and metal dispersion (D) of "fresh" catalysts, were carried out according to the procedure elsewhere reported [5,21]. The surface average Co particle size (d_{Co}), MSA and dispersion (D_{Co}) were evaluated on the basis of the following equations, assuming a spherical shape of the metal particle:

$$D_{Co}(\%) = \frac{((\mathrm{mol}_{H_2}/g_{cat}) \times PM_{Co} \times 100)}{\mathrm{Co(wt\%)}} \times 100$$

$$\mathrm{MSA}_{Co} = \frac{2 \times (\mu\mathrm{mol}_{H_2})}{g_{cat}} \times N_A \times \frac{10}{\sigma_{Co}}$$

$$d_{Co} = \frac{60 \times \mathrm{Co(wt\%)}}{\mathrm{MSA} \times \rho_{Co}}$$

where "σ_{Co}" represents the cross section of Co (6,5 Å^2/at), "ρ_{Co}" is the Co density (8,9 g/cm^3), while "N_A" is Avogadro's number.

Temperature Programmed Reduction (TPR) measurements in the range 373–1273 K were performed in a continuous flow apparatus using a linear quartz micro-reactor (i.d., 4 mm), loaded with 40 mg of samples, fed with a 6% H_2/Ar mixture flowing at 60 stp mL/min and heated at the rate of 15 K/min. The H_2 consumption was monitored by a TCD quantitatively calibrated with a commercial (Carlo Erba) CuO standard [5,19]. Prior to each run, samples were treated "in situ" at 673 K for 30 min in flowing O_2 (30 stp cm^3/min).

Transmission Electron Microscopy (TEM) analysis of "fresh" and "used" catalysts has been performed using a PHILIPS CM12 instrument provided with a high resolution (HR) camera for acquisition and elaboration of TEM images. Specimens were prepared by ultrasonic dispersion of catalyst samples in isopropyl alcohol depositing a drop of suspension on carbon supported films.

Scanning Electron Microscopy (SEM) analysis was performed using a *PHILIPS FEG XL-30 instrument*. SEM micrographs have been taken after coating the TLC samples with gold-film by sputtering method.

CHNS (Carlo Erba instrument) and TGA/DSC (Netzsch STA 409 analyzer) analysis were performed to evaluate the amount and quality of coke deposited on catalysts during reaction.

2.3. Catalyst testing

Catalytic tests were carried out using a Multilayer Reactor (MLR) elsewhere reported [19,20]. It consists of a quartz tube (F_{int}, 39 mm; length, 600 mm) provided with two metal flanges grooved to house the O-ring which ensured the sealing to the quartz reactor. Up to six TLCs samples were sandwiched between quartz discs (F_{ext}, 37 mm; thickness, 4 mm), used as spacers, and loaded into the reactor. An electrical heating oven, purposely designed to homogenously heat the reactor was used. Reaction temperature was controlled by using two thermocouples positioned inside the reactor just before the first TLC sample (inlet gas temperature) and on the external middle zone of the reactor. Experiments were performed at atmospheric pressure using CH_4/N_2/Ar reaction mixture in the molar ratio 2/1/17, flowing at 250 stp cm^3/min. The reaction stream was analyzed on-line by micro-GC Agilent 3000A equipped with two columns (Molecular Sieve 5 Å and OV-1) and two TC detectors. Prior to each run TLC samples were reduced "in situ" at 773 K for 1 h in flowing H_2 (150 stp cm^3/min).

3. Results and discussion

The main physical–chemical properties of "fresh" catalysts are reported in Table 1. The results clearly indicate that almost all samples, characterized by the same metal loading, are very similar in terms of surface area (about 45–60 m^2/g); only the Mo modified Co catalyst presents a SA significantly lower. In terms of metal dispersion the 20NiS sample is characterized by a higher metal surface area (about double respect to the other samples) and consequently by a smaller particle size diameter (14 nm against 17.2, 18 and 33 nm of 20NiAS, 20CoAS and 20CoS, respectively).

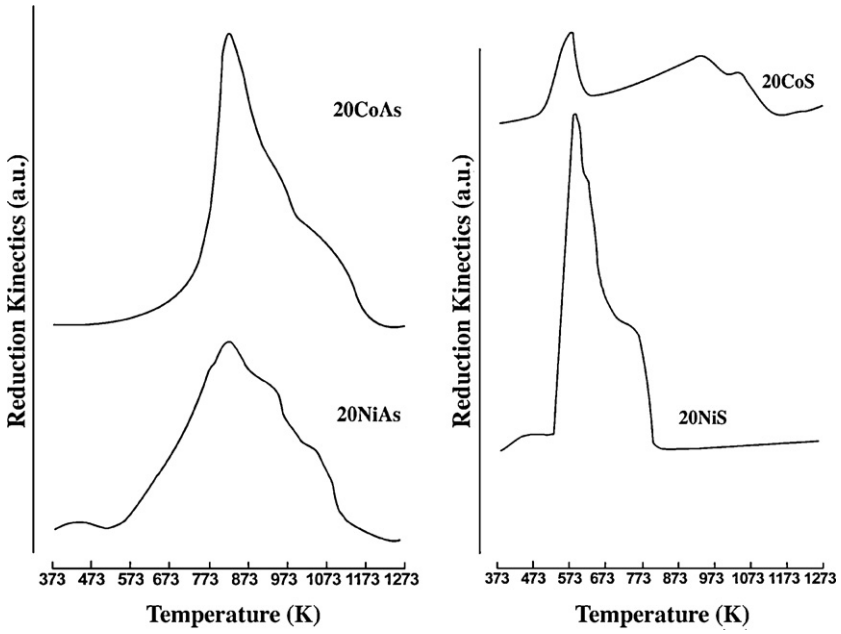

Fig. 1. TPR pattern of Ni/SiO_2, Co/SiO_2, Ni/Al_2O_3 and Co/Al_2O_3 silica cloth catalysts.

In Fig. 1 the TPR analysis carried out to highlight the reduction pattern of the various catalysts and to settle a proper activation (reduction) protocol for catalyst testing is shown. It can be seen that 20CoAS sample (Co/Al_2O_3) display a reduction pattern characterized by a main reduction peak at T_M = 773–953 K imputable to the reduction of CoO_3O_4 to Co^{2+} and the peak at T_M = 1063–1116 K is assignable to the reduction of bulk Co^{+2}, strongly interacting with support, to Co^0 [23,24]. The close similarity of the TPR profiles of such systems (20CoAS and 20NiAS) suggests that both metals (Ni and Co) have a comparable affinity for alumina and strongly bonds on catalyst surface. As regard the Ni supported catalyst, it is remarkable that, due to the formation of nickel surface aluminate [25] there is a fraction of nickel reducible only at high temperature (>1000 K).

On the contrary, a significant difference has been observed in case of silica supported Ni and Co samples. In particular the degree

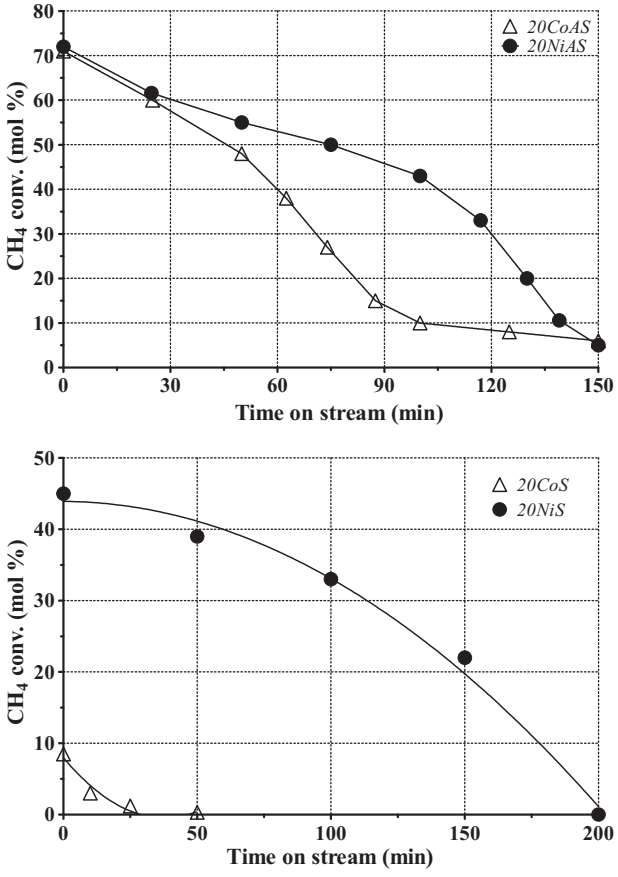

Fig. 2. Methane conversion *vs.* time on stream using 20NiAS, 20CoAS, 20NiS and 20CoS thin layer catalysts as a function of reaction time at 0.1 MPa and GHSV = 1900 h^{-1}.

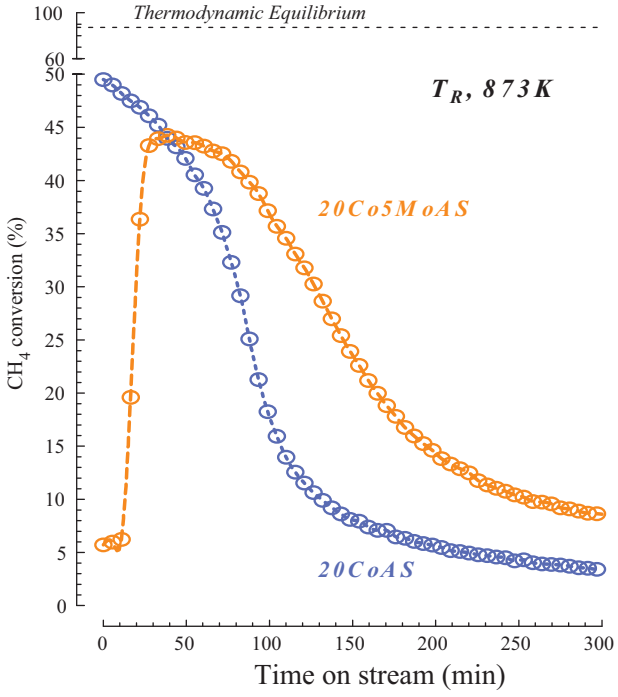

Fig. 3. Methane conversion *vs.* time on stream using 20CoAS and 20Co5MoAS systems.

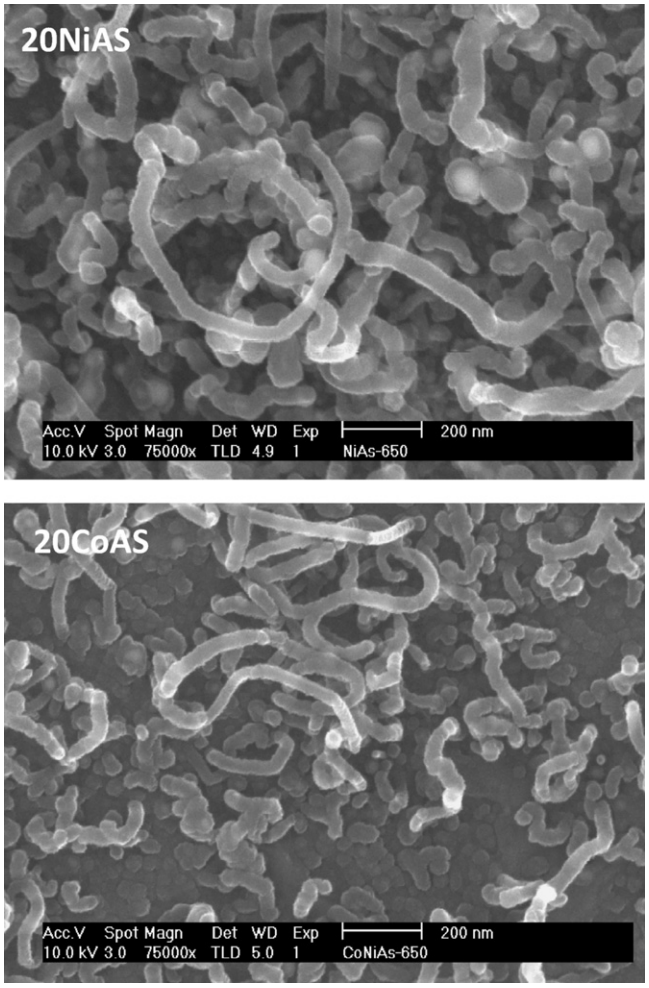

Fig. 4. SEM images of 20NiAS and 20CoAS used samples.

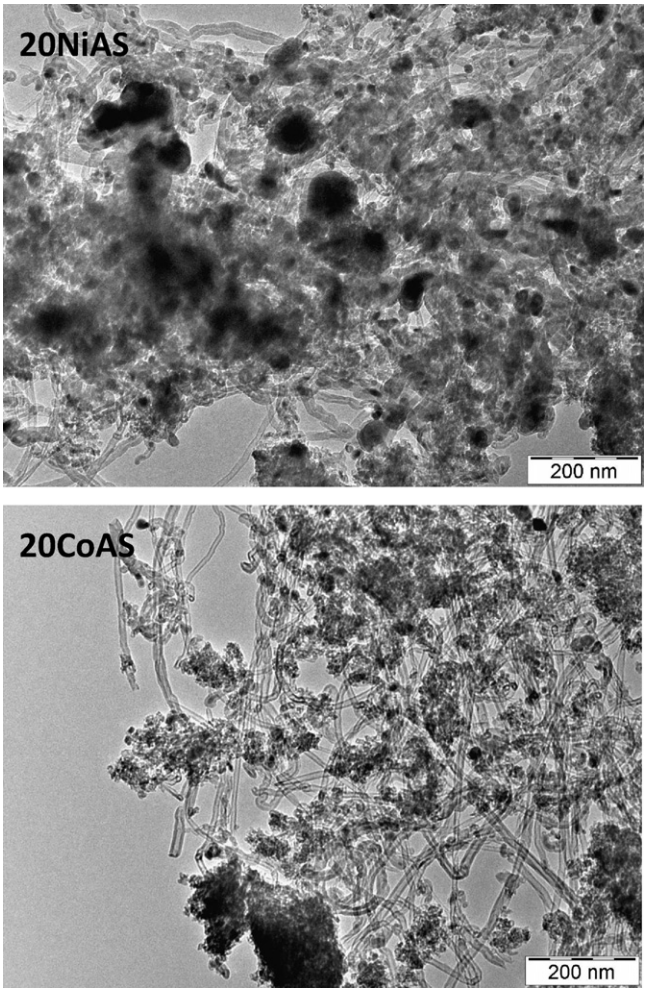

Fig. 5. TEM images of 20NiAS and 20CoAS used samples.

of reducibility of Co catalyst resulted to be much lower than Ni ones due a much stronger interaction of Co with silica.

The catalytic features of both Co and Ni based catalysts, in terms of methane conversion as a function of time, is shown in Fig. 2. Further to see that independently of reaction temperature investigated, both Ni and Co catalysts deactivate with time, by operating at low temperature (823 K) the initial activity of Co/SiO_2 catalyst (20 CoS sample) is much lower than the respective Ni/SiO_2 catalyst (8% against 45%) and furthermore it deactivates much faster. This result can be justified considering the TPR results shown in Fig. 1 from which it can be deduced that the amount of reduced Ni present on catalyst surface is much higher respect to the Co ones, therefore Ni catalyst resulted to be much active. At higher temperature (923 K) was not possible to perform experiments using Ni and Co on SiO_2 based catalysts since they deactivate in few minutes due to the formation of huge amount of encapsulating coke. On the contrary, interesting results were obtained at 923 K using Ni and Co supported on Al_2O_3. Further to observe that the initial activity is much higher (methane conversion close to 72% for both catalysts against 9 and 45% obtained using NiS and CoS samples, respectively), the deactivation of Co catalyst is much slower even if the Ni catalyst continues to be more stable on the time. Considering that both catalysts lost the activity at the same time (after 150 min), by using NiAS sample a H_2 productivity higher than about 35% was obtained.

In order to enhance the performance of Co based catalyst, following a survey of literature has been seen that the introduction of the Mo into formulation of the Co catalysts should contribute to improves its performance both in terms of hydrogen and nano-tube production [21]. Therefore, with the purpose to clarify if the best performance of the Co-Mo catalysts in comparison with Co system is imputable to electronic or geometry factor, we have carried out a comparative test at 873 K.

The activity/deactivation profile of 20CoAs and 20CO5MoAS systems, in terms of methane conversion *vs* the time on stream is shown in Fig. 3. The conversion profile underline for 20Co5MoAS system a period of induction (30 min) in which the conversion of the methane quickly increases from 5% to 45%. This could be attributable to the partial reorganization/activation of the catalytic surface due to the carburization of the Mo (Mo_2C) [26]. After that catalyst deactivates but with a much lower rate respect to the unpromoted Co/Al_2O_3 catalyst. Considering that both the systems are similar in terms of MSA, D_{Co} and d_{Co}, it can be hypothesized that the Mo acts as electronic promoter avoiding the formation on active sites of encapsulating carbon. The carbon capacity (C/Co) of the system 20Co5MoAS calculated on the base of the results brought in Fig. 3 resulted to be close to 23.6, about 2.5 times higher than that obtained by using bare 20CoAS sample.

From SEM and TEM images of 20CoAS and 20NiAS spent catalysts shown in Figs. 4 and 5 it can be observe how carbon filaments grow on catalyst surface entangled one another. It can be also seen that filaments formed on 20NiAS sample are larger and longer respect to that formed on 20CoAS sample. This result can be justified referring to the TEM results shown in Fig. 5. In fact, Ni on

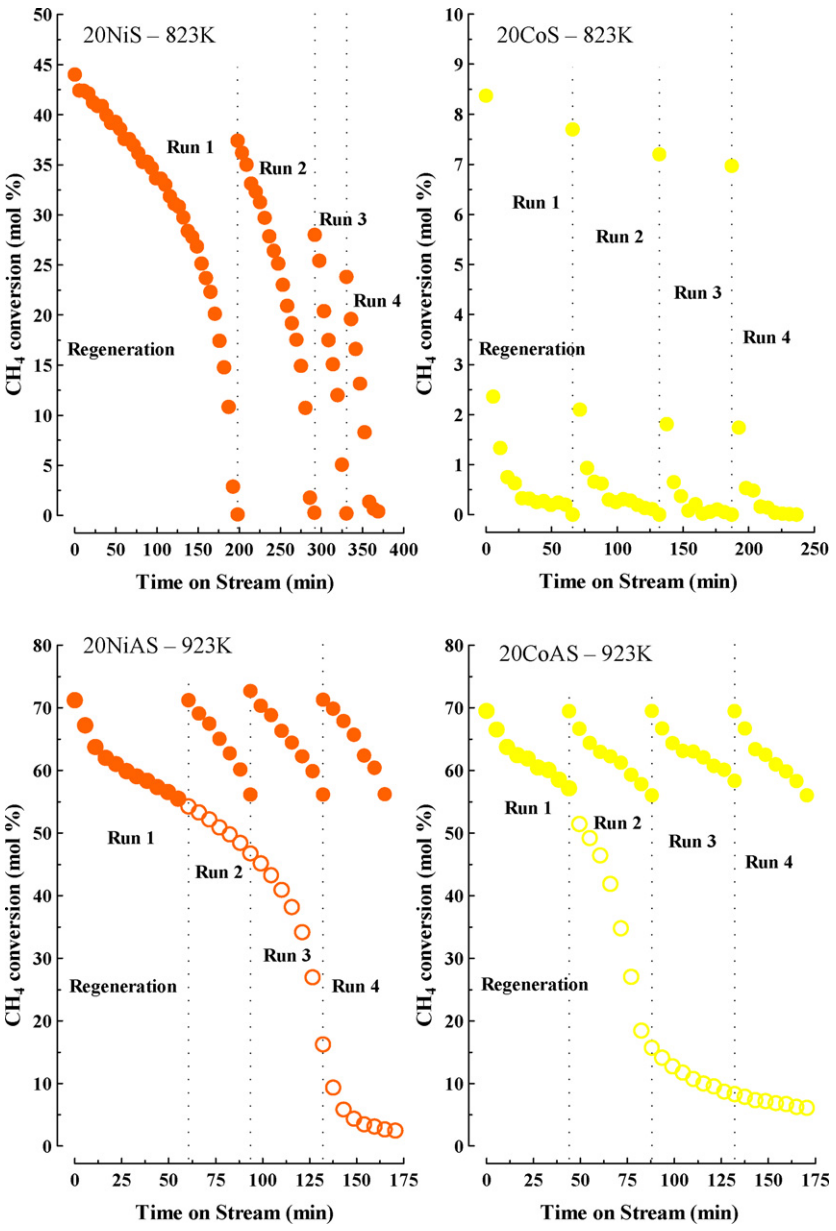

Fig. 6. Catalytic behaviour of Ni and Co TLC catalysts at 823 and 923 K in a dual-step process: methane conversion as a function of time after catalyst regeneration in oxygen stream. (○) represent the conversion profile of run carried out without regeneration.

the contrary of Co, is subjected to sintering with the consequence of favouring the formation of bigger filaments. TEM images also show that the larger Ni particles are affected by the formation of "encapsulating" carbon that, as previously reported [19] drastically contribute to deactivate the catalyst. On the contrary, Co catalyst result to be much resistant to sintering (see Fig. 6B), in fact metal particles do not significantly enlarge during reaction and carbon filaments result to be both smaller in size and more homogeneously distributed on catalyst surface.

These results confirm that the nature and strength of metal–support interaction play a fundamental role in determining what kind of carbon formation mechanism is preeminent.

In order to evaluate the behaviour of Ni and Co catalysts in a cyclic two step process based on catalyst regeneration by oxygen treatment, a series of experiments have been carried out at different reaction temperature: 823 and 923 K, respectively. Prior to each run the oxidised catalyst, after regeneration in oxygen, was reduced in hydrogen flow.

From the result shown in Fig. 6 it clearly emerge that at 823 K both silica supported Ni and Co catalysts lost activity with cycles. This evidence is due to the type of coal formed during reaction. In fact, on these systems characterized by low MSI, carbon filaments with metal particles on top normally form. This, as previously reported, is deleterious for catalyst since the particles detach from catalyst surface and during oxidation step, when the filament is burned the Ni particle fall down to the bottom of the reactor and catalyst loses its activity.

Ni and Co supported alumina catalyst behave differently and have no problems with cycles, in fact, the initial activity is recovered after oxidation and the deactivation trend of each cycle does not change significantly. This interesting result is due to the strong interaction between metal and support (alumina) that is established during calcination (see Fig. 1). For this reason, as previously vindicated, for NGCD reaction the strong metal support interaction is fundamental prerequisite to ensure that during reaction the active metal remain well anchored on support surface [27]. Recent

results [28] clearly vindicate that in case of strong MSI carbon atoms are released due to decomposition of the metastable CxNiy intermediate in the other side of the exposed surface of the Ni particle and the nanotubes are constructed in the surface of the Ni particle towards gas–solid interface. As the result, the Ni particle is fixed in the support but leaving carbon tube growing with a closed end.

3.1. Modelling of deactivation mechanism

The CDNG reaction was extensively studied in the last decades, and in particular the nickel based catalysts have revealed the best performance both in terms of activity and stability. However, the main technological drawbacks, associated with catalyst coking and decoking remain still unsettled limiting the industrial exploitation of such potential technology.

In previous papers [19,21], we have recognized that the use of a structured multilayer reactor (MLR) constituted by a set of nickel thin layer catalysts avoids the reactor plugging allowing CDNG operations under quasi-isothermal conditions. The nickel based catalysts, though very active in the CDNG in the range 773–873 K, do not allowed reversible cyclic stepwise operations because of the tip growth coking mechanism which implies the loss of active species during the catalyst decoking.

In order to discriminate the contribution of coking and sintering phenomena a modelling of the deactivation pattern has been proposed. Initially, we have postulated that the CDNG reaction needs two active sites, such hypothesis is confirmed correlating the rate of studied catalysts (T_R, 773 K) with theirs MSA × MSA, defined θ^2: the result is a straight line correlation (Fig. 7). Therefore, considering θ proportional to active site, it has been postulated the following surface reaction pathway for CDNG reaction:

$$CH_4 + \theta \rightleftarrows CH_4\text{-}\theta$$

$$CH_4\text{-}\theta + \theta \rightarrow CH_3\text{-}\theta + H\text{-}\theta \text{ r.d.s.}$$

$$CH_3\text{-}\theta + \theta \rightleftarrows CH_2\text{-}\theta + H\text{-}\theta$$

$$CH_2\text{-}\theta + \theta \rightleftarrows CH\text{-}\theta + H\text{-}\theta$$

$$CH\text{-}\theta + \theta \rightleftarrows C\text{-}\theta + H\text{-}\theta$$

$$2H\text{-}\theta \rightleftarrows H_2 + 2\theta$$

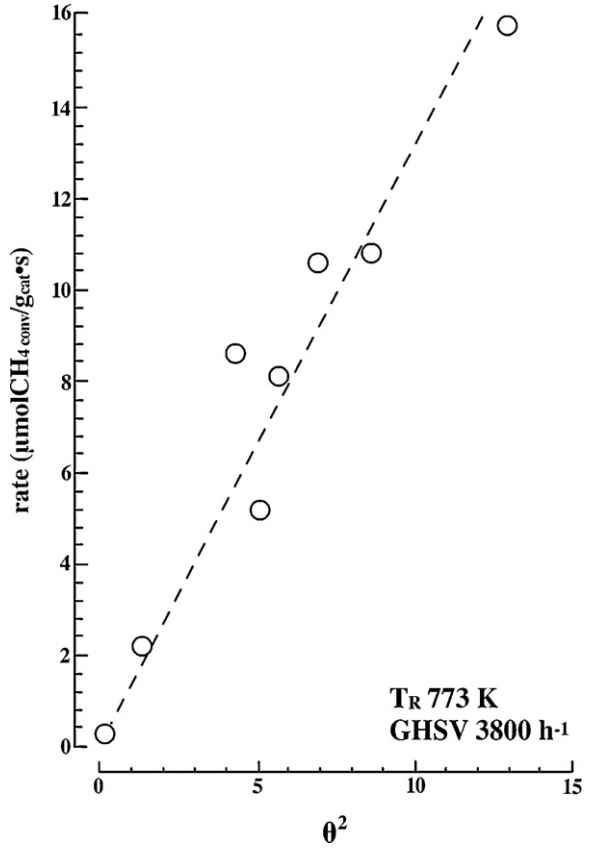

Fig. 7. Correlation between initial reaction rate, obtained using Ni based catalysts, and surface site coverage, θ^2.

For the modelling of deactivation pattern it has been postulated that the deactivation rate is proportional to the rate of active site coverage. Considering at t_0 the site is not coverage and then the relative activity, α, equal at 1 (defined as CH_4 conversion at $t_{i\text{-esimo}}$ ratio CH_4 conversion at t_0), the number of active site covered is 1-α, defined γ. Therefore, on what postulated, the deactivation rate is defined as follow:

$$\frac{d\theta}{dt} = (k_{SINT} + k_{COK}) \times \theta^2 t \cdot \frac{d\theta}{dt} = (K_{SINT} + K_{COK}) \times \theta^2 t$$

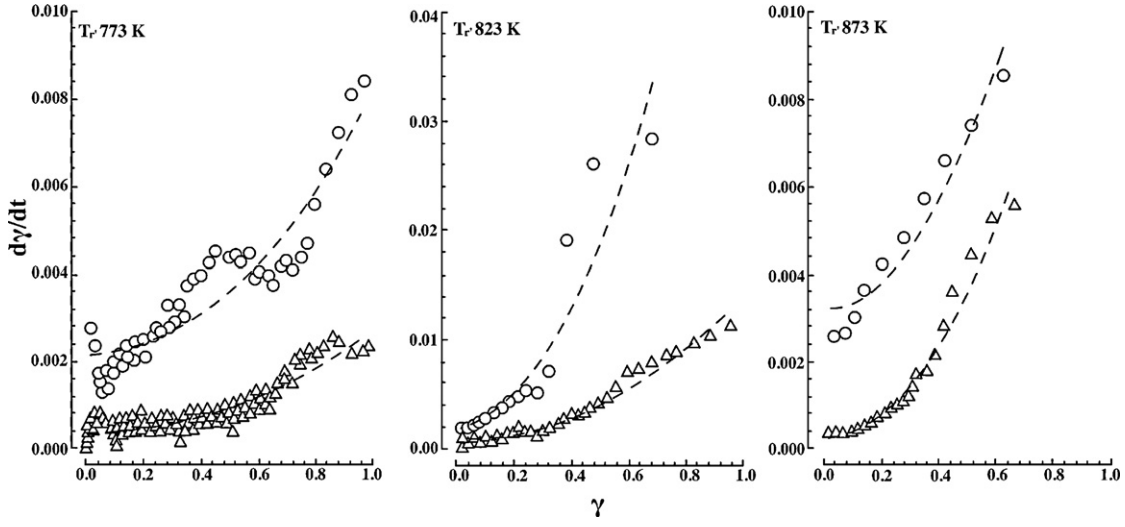

Fig. 8. Correlation between calculated and experimental data obtained using (○) NiS and (△) MNiS catalysts.

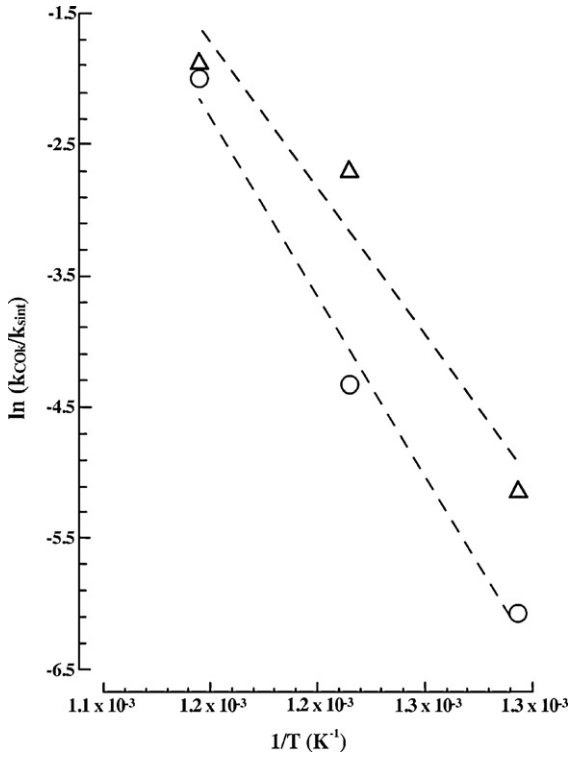

Fig. 9. Relationship between deactivation rate and temperature. (○) NiS and (△) MNiS.

In order to validate such deactivation modelling data obtained using two different Ni based catalysts, different influenced by sintering phenomena, have been used. In particular, 20NiS sample was strongly influenced by sintering phenomena increasing reaction temperature, whereas MNiS sample was poorly influenced by sintering phenomena due to the presence of MgO which prevent the surface migration of Ni particles [14,20].

The results shown in Fig. 8 clearly demonstrate that the proposed model is reliable regardless of the reaction temperature investigated.

In order to discriminate the role of sintering and coking on the deactivation pattern it has been calculated the activation energy of deactivation rate for the studied systems. From the results obtained (see Fig. 9) it can be drawn that for the 20NiS system the main deactivation phenomena is sintering, whereas for MNiS is coking. These results demonstrate that the sintering phenomena prevail on coking deactivation phenomena when the metal–support interaction is very low (this is the case of 20NiS sample), causing the arising of sintering phenomena.

Therefore, the deactivation pattern was regulated by sintering and coking phenomena, but the sintering is inhibits by the high metal–support interaction, denoting a main deactivation rate on the catalysts subjected to sintering phenomena [5,14,19,20].

4. Conclusions

The performance of a structured Multilayer Reactor (MLR) and a series of Ni and Co silica and alumina Silica Cloth Thin Layer Catalysts in the CDNG reaction for the production of "CO_x-free" H_2 in the T_R range 773–973 K has been assessed.

The results clearly reveal that the nature and strength of metal–support interaction is the basis for developing an efficient catalyst for the decomposition reaction of methane. In particular, it was observed that the alumina is better suited support than the silica as it allow to prepare Ni and Co based catalysts characterized by a strong MSI. This peculiarity is fundamental to operate at high temperatures, with high conversion of methane without significant changes of catalysts structure. However, Co/Al_2O_3, even though presented a lower activity than the Ni/Al_2O_3 was more stable from structural point of view and was not subject neither to formation of "encapsulating" carbon nor to the sintering. With both Ni and Co alumina supported TLC samples has been possible to demonstrate that MLR is a suitable tool to realize a dual-step process based on CDNG reaction and O_2-regeneration.

The deactivation model proposed resulted to be a reliable tool to discriminate the contribution of sintering and coke formation on catalyst deactivation.

References

[1] Enea in: Idrogeno, Energia del futuro G23-031-0-0, October 2003.
[2] R.F. Service, DARWIN Nov/Dic (2004) 18.
[3] G. Marbán, T. Valdés-Solis, Int. J. Hydrogen Energy 32 (2007) 1625.
[4] N. Muradov, Int. J. Hydrogen Energy 18 (1993) 211.
[5] G. Italiano, C. Espro, F. Arena, F. Frusteri, A. Parmaliana, Stud. Surf. Sci. Catal. 162 (2006) 633.
[6] D. Chen, R. Lødeng, A. Anundskás, O. Olsvik, A. Holmen, Chem. Eng. Sci. 56 (2001) 1371.
[7] S. Takenaka, H. Ogihara, I. Yamanaka, K. Otsuka, Appl. Catal. A: Gen. 217 (2001) 101.
[8] B. Monnerat, L. Kiwi-Minsker, A. Renken, Chem. Eng. Sci. 56 (2001) 633.
[9] L.B. Avdeeva, O.V. Goncharova, D. Kochubey, V. Zaikovskii, L.M. Plyasova, B.N. Novgorodov, S.K. Shaikhutdinov, Appl. Catal. A: Gen. 141 (1996) 117.
[10] L.B. Avdeeva, D. Kochubey, S.K. Shaikhutdinov, Appl. Catal. A: Gen. 177 (1999) 43.
[11] M.A. Ermakova, D. Yu Ermakov, G.G. Kuvshinov, Appl. Catal. A: Gen. 201 (2000) 61.
[12] S. Takenaka, Y. Tomikubo, E. Kato, K. Otsuka, Fuel 83 (2004) 47.
[13] T.V. Choudhary, C. Sivadinarayana, A. Klinghoffer, D.W. Goodman, Stud. Surf. Sci. Catal. 136 (2001) 197.
[14] G. Italiano, C. Espro, F. Arena, F. Frusteri, A. Parmaliana, Catal. Lett. 124 (2008) 7.
[15] N.Z. Muradov, F. Smith, A. T-Raissi, Catal. Today 103–103 (2005) 225.
[16] L.B. Avdeeva, D.I. Kochubey, S.K. Shaikhutdinov, Appl. Catal. A 177 (1999) 43.
[17] Z. Zhong, H. Chen, S. Tang, J. Ding, J. Lin, K. Lee Tan, Chem. Phys. Lett. 330 (2000) 41.
[18] M. Wietschel, U. Hasenauer, Renewable Energy 32 (2007) 2129.
[19] G. Italiano, C. Espro, F. Arena, F. Frusteri, A. Parmaliana, Appl. Catal. A: Gen. 357 (2009) 58.
[20] G. Italiano, C. Espro, F. Arena, A. Parmaliana, F. Frusteri, Appl. Catal. A: Gen. 365 (2009) 122.
[21] S.P. Chai, S. Hussein, S. Zein, A.R. Mohamed, Appl. Catal. A: Gen. 326 (2007) 173.
[22] S.P. Chai, S.H. Zein, M. Sharif, A.R. Mohamed, Chem. Phys. Lett. 426 (2006) 345.
[23] P. Arnoldy, J.A. Moulun, J. Catal. 93 (1985) 38.
[24] C.L. Bianchi, Catal. Lett. 76 (2001) 155–159.
[25] J. Juan-Juan, M.C. Romàn-Martínez, M.J. Illán-Gómez, Appl. Catal. A: Gen. 264 (2004) 169–174.
[26] J.S. Rieck, A.T. Bell, J. Catal. 96 (1985) 88.
[27] G. Italiano, A. Delia, C. Espro, G. Bonura, F. Frusteri, Int. J. Hydrogen Energy 35 (2010) 11568–11575.
[28] J.C. Guevara, J.A. Wang, L.F. Chen, M.A. Valenzuela, P. Salas, A. García-Ruiz, J.A. Toledo, M.A. Cortes-Jácome, C. Angeles-Chavez, O. Novaro, Int. J. Hydrogen Energy 35 (2010) 3509–3521.